
Flash-VL 2B: Optimizing Vision-Language Model Performance for Ultra-Low Latency and High Throughput

Bo Zhang Shuo Li Runhe Tian Yang Yang Jixin Tang Jinhao Zhou Lin Ma

Meituan

Abstract

In this paper, we introduce Flash-VL 2B, a novel approach to optimizing Vision-Language Models (VLMs) for real-time applications, targeting ultra-low latency and high throughput without sacrificing accuracy. Leveraging advanced architectural enhancements and efficient computational strategies, Flash-VL 2B is designed to maximize throughput by reducing processing time while maintaining competitive performance across multiple vision-language benchmarks. Our approach includes tailored architectural choices, token compression mechanisms, data curation, training schemes, and a novel image processing technique called implicit semantic stitching that effectively balances computational load and model performance. Through extensive evaluations on 11 standard VLM benchmarks, we demonstrate that Flash-VL 2B achieves state-of-the-art results in both speed and accuracy, making it a promising solution for deployment in resource-constrained environments and large-scale real-time applications.

1 Introduction

The rapid advancements in Vision-Language Models (VLMs) have led to significant breakthroughs in multimodal understanding, enabling systems to integrate visual and textual information for a variety of applications such as image captioning, visual question answering, and cross-modal retrieval. Recent models, including LLaVA [41, 40], Qwen-VL [4, 78], Intern-VL [10, 9], and MobileVLM [11, 12], have pushed the boundaries of performance by scaling model sizes and refining architectures. These models have set new benchmarks, demonstrating significant accuracy improvements across multiple vision-language tasks. However, as model complexity increases, there is a critical need to address the trade-off between performance and computational efficiency, particularly for real-time and resource-constrained environments.

Despite their remarkable accuracy, existing state-of-the-art VLMs often face challenges in deployment due to their high latency and computational demands, limiting their applicability in applications requiring fast and scalable inference. For example, recent VLMs support dynamic resolution either by splitting images into finer patches [10] or resizing to the nearest size to facilitate downsampling [78], hence substantially increasing the number of visual tokens for LLMs to process. In practice, both approaches increase visual encoding latency as well as the duration of the decoding stage. DeepSeek-VL2 [79] leverages mixture-of-experts as LLMs to enhance performance, however the sparse MoE architecture naturally requires more memory access, which hinders the inference speed.

To bridge this gap, we propose Flash-VL 2B, a new VLM architecture designed to achieve ultra-low latency and higher throughput without sacrificing accuracy. By incorporating cutting-edge architectures, novel tiling strategies, token compression techniques, and advanced data and training

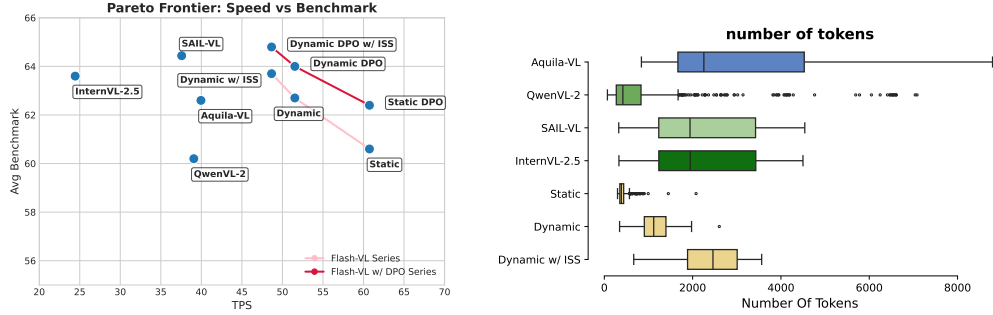


Figure 1: **Left:** Pareto front of VLMs in terms of the average accuracy on 11 standard VLM benchmarks and the TPS (tokens per second). **Right:** The distribution of the input token numbers processed by the LLM component of each VLM given various image sizes of the MMMU dataset.

schemes, Flash-VL 2B aims to provide a more efficient alternative to current VLMs, particularly for applications that require fast real-time performance and scalability. In this work, we demonstrate that Flash-VL 2B not only delivers state-of-the-art accuracy on common VLM benchmarks but also provides significant improvements in speed and throughput (up to 60.73 tokens/s in Figure 1 left), making it a promising candidate for deployment in both cloud and edge environments. Our Flash-VL-2B series has a higher compression on the number of total tokens, faster than its counterparts, while being better or on par in average performance on 11 standard VLM benchmarks.

2 Related Work

The prominent VLMs so far generally adopt a ViT-Adapter-LLM architecture disseminated by LLaVA [41]. For an efficient design of VLMs, the choice of visual encoders [15] and LLMs incurs a critical trade-off between strength and efficiency.

Vision Encoders. Contrastive language-image pretraining [57] has become the most powerful method for visual representation learning. By training over 400M image-text pairs with weak language supervision, CLIP [57] unlocks competitive ImageNet zero-shot accuracy and many other downstream tasks. Open-CLIP [21] lays more importance on data curation, releasing a massive filtered high-quality multi-modal dataset called DataComp-1B. Eva-CLIP [67] further boosts the performance by scaling training data to have 9B samples. Intern-ViT [10] scales ViTs to 6B to parallel the number of parameters of LLMs. DFN [18] emphasizes a filtering strategy of data curation and releases a new dataset DFN-5B filtered out of 12.8B CommonPool. Most recently, SigLIP [86] enhances CLIP by transforming the softmax-based contrastive loss to a sigmoid one. Its successor SigLIP2 [74] extends the training objectives to incorporate caption-based pretraining [76] and self-distillation as in DINOv2 [52]. AIM [17, 19] series is solely built on an autoregressive objective where the model generates the sequence of raw image patches and text tokens (added in AIMv2 by pairing a multimodal decoder). Among all, the SigLIP series achieves a nice trade-off between inference cost and performance, offering more compact but competitive models.

Lightweight LLMs. LLaMA series [72, 73, 22] provides a wide range of language models, where the smallest one of earlier versions has 7B parameters. To achieve ultra-low latency, pruning methods like LLM-Pruner [47] and [51] are introduced to nearly compress LLMs by half of the parameters. In contrast, others train smaller models from scratch, which has been proven to have higher compactness in terms of accuracy at the same scale. Phi series [25, 39, 1] targets phone use cases by training light-weight models on the high-quality textbook corpus. Gemma 2 [71] utilizes distillation to obtain smaller models. MiniCPM [29] studies the scaling law in extremely small LLMs and proposes a warmup-stable-decay training strategy for better convergence. Qwen [3, 80] ships a rich configuration of models equipped with architectural upgrades and trained on larger-scale data (up to 18T training tokens), whose smallest version serves as a very competitive base model for building up light-weight VLMs.

Efficient VLMs. LLaVA series [41, 40] illustrates a popular paradigm and also a training recipe for efficient VLMs. MobileVLM [11, 12] aims to increase the inference speed by compressing visual

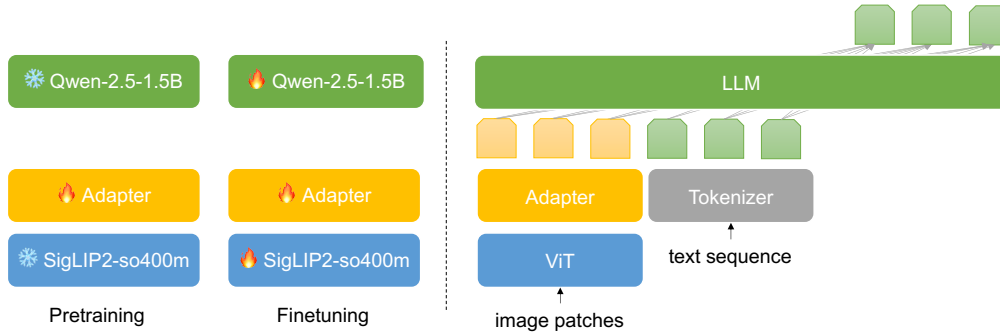


Figure 2: The Flash-VL architecture adopts a ViT-Adapter-LLM paradigm trained in multi-stages, striking an outstanding trade-off between accuracy and speed.

tokens via a light-weight adapter. Phi-4 [2] and Gemma 3 [70] are the multi-modal follow-ups built on their previous lightweight LLMs. NVILA [43] undertakes a “scale-then-compress” approach, which allows efficient processing of high-resolution images and long videos. FastVLM [75] makes use of a hybrid vision encoder to significantly reduce encoding time for high-resolution images. LLaVA-OneVision [33] comes with efficient VLMs that handle images, texts, and videos. Qwen-VL2 [78] proposes a dynamic resolution mechanism to process images of arbitrary size, it also unifies image and video representation by integrating 3D convolutions and multi-modal RoPE [66]. Aquila-VL [23] curates a 40M open-sourced multimodal dataset that significantly increases the training efficiency. Lately, SAIL-VL [14] enhances the data pipeline to produce scalable data where models can be trained based on the sample complexity via curriculum learning.

3 Flash-VL

3.1 The VLM Architecture

Following LLaVA [41], we choose a conventional ViT-Adapter-LLM setup for constructing our VLM. With inference requirements and compute budget in mind, we select SigLIP2-so400m-patch16-512 [74] by default for the vision encoder and Qwen-2.5-1.5B-Instruct [81] as our language model. These two major components are connected by a lightweight adapter with token compression done by pixel shuffling, as depicted in Figure 2.

Visual Encoder. For ultra-low latency and high throughput, we refrain from the common dynamic tiling strategy [9, 29] as it substantially induces computational costs. Among all available visual encoders, SigLIP2 [74] features fewer parameters at a lower fixed image resolution while trained at dynamic resolution scales. We compare SigLIP2 and AIMv2 [19] later in Table 3, manifesting the superiority of SigLIP2 in visual representation capacity. For each input image, we resize to 512×512 and slice out 32×32 patches each of size 16×16 , yielding 1024 visual tokens in total.

Adapter. To compress the number of visual tokens for efficiency, we adopt pixel shuffling [9] to swap every other two pixels in the H and W dimensions to the hidden dimension, effectively reducing the number of tokens by four times to have 256 tokens. Beyond that, we append layer normalization and linear layers with intermediate activations to align with the LLM. Formally, for given visual feature x , we process it as follows,

$$x = \text{PixelShuffle}(x) \quad (1)$$

$$x = \text{LayerNorm}(x) \quad (2)$$

$$x = \text{GELU}(\text{Linear}(x)) \quad (3)$$

$$x = \text{GELU}(\text{Linear}(x)) \quad (4)$$

$$x = \text{Linear}(x) \quad (5)$$

The comparison of this adapter with the conventional two MLP layers is in Table 8 of Section A.1.

Language Model. Among all dense lightweight models below 2B parameters, Qwen-2.5-1.5B-Instruct [81] boasts the best overall performance on various language tasks. It ships a potent causal LLM out-of-box with advanced architectural upgrades like SwiGLU [62], RoPE [66], RMSNorm [87], and tied word embeddings [55]. It also enables a large vocabulary of 151936 and a context length of 32K (including an 8K output length). We compare it with other LLM candidates later in Table 9 of Section A.2.

Dynamic Resolution Variants. To understand the upper limit of our architecture and pipeline, we also train VLMs with dynamic resolution schemes as a comparison. For such a purpose, we adopt a tiling strategy (Figure 3(b)) as in MiniCPM [29] and utilize AIMv2 [19] for the vision encoder. This dynamic setting demonstrates a better performance of the current data and training pipeline and illustrates the gap over the default fixed version.

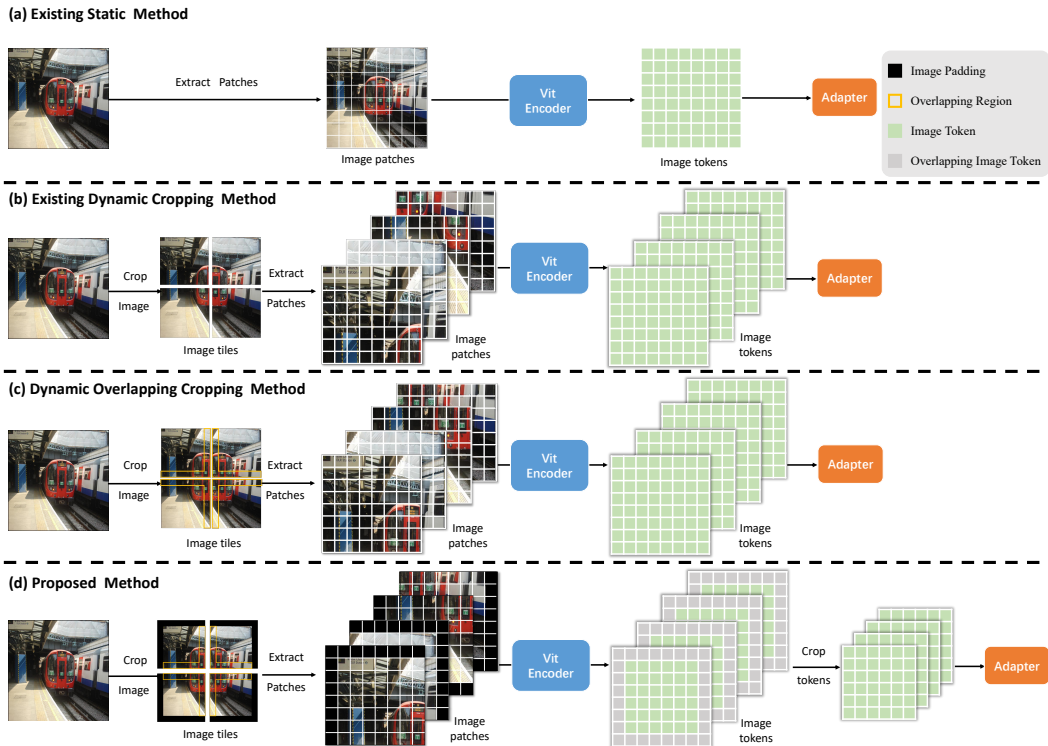


Figure 3: Image processing strategies in VLMs. (a) Static Method (b) Dynamic Cropping Method (c) Dynamic Overlapping Cropping Method (d) The Proposed Implicit Semantic Stitching.

Implicit Semantic Stitching. In addition, we discover that the scheme of Figure 3 (b) directly clips the semantically connected regions, breaking the semantic continuity among these image patches. To mitigate this semantic discontinuity effect, a rather straightforward idea is to adopt overlapping alongside cropping as shown in Figure 3 (c). Surprisingly, the inclusion of a large amount of repetitive information can degrade the performance, as detailed later in the ablation experiment in Section 4.8.

To address this issue, we propose *Implicit Semantic Stitching* (ISS), which extracts image tiles’ boundary consensus features as a type of inter-tile semantic glue, ensuring semantic consistency without sacrificing dynamic cropping benefits. As shown in Figure 3 (d). We first pad the input image with a black frame to facilitate cropping. Then for image cropping, we reuse the overlapping scheme. After extracting the visual features, we remove the overlapping image tokens (the gray ones represent overlapping tokens, and the green ones represent retained tokens). Although all the visual tokens in the first image tile do not explicitly include boundary tokens from the second image tile, the boundary features of the second tile are implicitly incorporated via feature embedding. Metaphorically speaking, ISS stitches together the cutting-off semantic regions. The parameter details of the method are shown

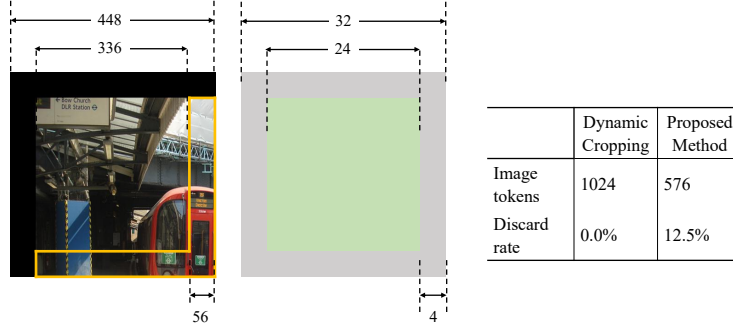


Figure 4: Implicit Semantic Stitching. **Left:** An example of one image tile and its feature map, where the yellow box represents the repetitive areas. The gray area represents the overlapping tokens, and the green ones represent retained tokens. **Right:** The overlap rate is approximately 12.5%; The number of image tokens of each image tile is 576.

in Figure 4, the maximum number of image tile of one inputs image is limited to 4, for one image tile, the overlap rate is approximately 12.5%, the number of image tokens is 576.

3.2 Data Choices

Data curation has been one of the core advances for VLM’s performance. Among the large-scale open-source multimodal dataset collections available, LLaVA-One-Vision [33] and InfinityMM [23] are the most prominent due to both quantity and quality. VLMs trained on them showed distinguished performance. To facilitate the reproducibility of our models, we build Flash-VL on InfinityMM (Stage 1 to 3) along with an independent Stage 4 constructed by assembling a large set of open-source datasets shown in Table 6 and Figure 5. The preference dataset used in Stage 5, approximately 87k, is mainly curated from [36] along with some partial in-house data.

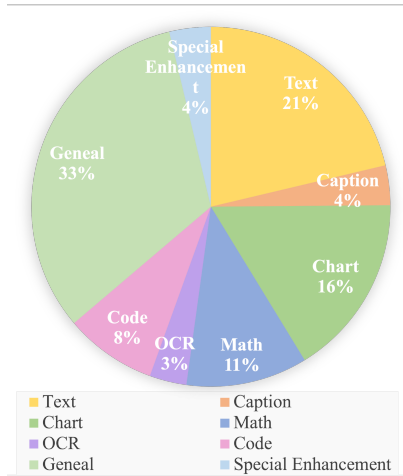


Figure 5: Pie chart of the Stage 4-10M data categorized by General, Code, OCR, Math, Chart, Caption, Text, and Special enhancement.

Data Source	Type
ShareGPT4V[6]	Caption
ChartQA[48]	Chart
DocVQA[50]	Chart
InfographicVQA[49]	Chart
Deepform[68]	Chart
Kleister[65]	Chart
TabFact[8]	Chart
WikiTableQuestions[53]	Chart
VisualMRC[69]	Chart
TextCaps[63]	Chart
TextVQA[64]	Chart
ScigraphQA[38]	Chart
MultiMath[54]	Math
MAVIS[89]	Math
DocStruct4M[27]	OCR
Websight[32]	Code
MMDU[44]	General
M4Instruct[35]	General
M3IT[37]	General
ALLaVA[26]	General
ShareGPT-4o[59]	Special Enhancement

Figure 6: Multi-modal Data sources of Stage-4.

3.3 Training Strategies

Our Flash-VL follows a multi-stage training pipeline, see Table 1. During Stage 1, only the Adapter is set to be learnable to align vision representations with textual embeddings, and the learning rate

decays from $1e-3$ to $2e-5$. For the Stage 2 to 4, all parameters are active for training and have a cosine annealing from $1e-5$ to zero. All data samples are seen only once. For Stage 5, we adopt Direct Preference Optimization (DPO) [58] with LoRA [28] only on the LLM and the Adapter.

	Stage 1	Stage 2	Stage 3	Stage 4	Stage 5
Train Phase	Pre-train	Fine-tune	Fine-tune	Fine-tune	DPO
Resolution	512	512	512	512	512
Data Samples	10M	24M	6M	10M	87k
Trainable	Adapter	Full Model	Full Model	Full Model	LLM+Adapter
Train Type	Full	Full	Full	Full	LoRA
Trainable Params	91.02M	1733.07M	1733.07M	1733.07M	10.73M
LR Schedule	Cosine Decay				
LR	$1.00E-03$	$1.00E-05$	$1.00E-05$	$1.00E-05$	$1.00E-05$
LR _{min}	$2.00E-05$	0	0	0	0
Epoch	1	1	1	1	1

Table 1: Configuration for training Flash-VL-2B across various stages.

4 Experiments

4.1 Setup

Ablation Setting. For ablation studies, we pretrain the models on a 2.5M combined samples of ShareGPT4V-PT-1246K [6], ALLaVA-Caption-710K [5], LLaVA-CC3M-Pretrain-595K [41], and then finetune them on the LLaVA-1.5-665K [40] dataset. The pretraining takes $8 \times$ A100 GPUs to train, with a global batch size of 48, an initial learning rate of $1e-3$, a minimum learning rate of $2e-5$, and 400 steps of warm-ups. Finetuning starts with a learning rate of $1e-5$ and decays to zero with cosine annealing. All data samples are seen only once.

Benchmarks. We evaluate our models and the state-of-the-art lightweight VLMs on a myriad of multimodal benchmarks such as MMMU [84], MMBench [83], MMStar [7], MMVet [82], MathVista [46], AI2D [30], HallusionBench [24], OCRBench [42], MME [20], SEEDBench [34]. For multimodal reasoning capacity, we evaluate on DynaMath [90], MathVision [77], MathVerse [88], MMMU Pro [85], WeMath [56]. We adopt VLMEvalkit [16] for the evaluation purpose of all models.

Full Pipeline Setup. Table 1 gives the hyperparameters for our complete pipeline training. For stage 5, we grid search the β of DPO to find 0.1 gives the best performance. It comprises five stages. We train our models on $40 \times$ A100-80G GPUs with a global batch size of 240. Note we choose SigLIP2-so400m for the static resolution version and AIMv2 H/14448 for the dynamic variants as we find the dynamic version of AIMv2 shows better performance than SigLIP2 under the ablation setting, see Table 10 of Section A.3.

4.2 Comparison of state-of-the-art lightweight MLLMs

Table 2 gives the comparison with Qwen2-VL, InternVL2.5, and Aquila-VL (all in the range of 2B parameters) on 11 common VLM benchmarks. These benchmarks span a wide range of categories, seeking to ensure a rigorous and balanced evaluation of Flash-VL’s performance in various multimodal tasks. First, as shown in Table 2, Flash-VL-2B_{d-ISS} surpasses previous state-of-the-art method InternVL2.5-2B by 1.2% on average. Specifically, on MathVista, Flash-VL-2B_{d-ISS} outperforms the previous state-of-the-art method Aquila-VL-2B by 2.1%. On OCRBench, Flash-VL-2B_{d-ISS} outperforms the previous state-of-the-art method InternVL2.5-2B by 43. These results showcase the ability of Flash-VL-2B_{d-ISS} to handle general multimodal understanding and reasoning tasks. Second, Compared with Flash-VL-2B_d, Flash-VL-2B_{d-ISS} improves it by 3.4%, 3.5%, 12 and 0.8% for MathVista_{testmini}, HallusionBench, OCRBench, and average of 11 benchmarks respectively, which demonstrates the advantage of the ISS technique in enhancing general multimodal tasks. Third, Flash-VL-2B_s with higher throughput outperforms Qwen2-VL-2B on average of 11 benchmarks by 2.2%. For instance, Flash-VL-2B_s delivers significant gains on MMBench^{en} (78.4 vs. 74.9), MMStar (53.8 vs. 48.0), and MathVista_{testmini} (59.3 vs. 43.0), these results further indicate the great potential of Flash-VL-2B_s.

Benchmark	Qwen2-VL-2B	Aquila-VL-2B	InternVL2.5-2B	Flash-VL-2B _s	Flash-VL-2B _d	Flash-VL-2B _{d-ISS}
MMMU _{val}	41.9	44.4	41.8	43.6	42.9	42.9
MMBench ^{en}	74.9	78.6	74.7	78.4	78.4	79.1
MMBench ^{cn}	73.5	76.3	71.6	74.7	74.9	76.7
MMStar	48.0	54.9	54.1	53.8	54.4	54.1
MathVista _{testmini}	43.0	59.4	50.9	59.3	58.1	61.5
AI2D _{test}	74.1	75.0	75.1	74.2	74.1	74.4
MMVet	49.5	40.9	61.7	47.3	52.7	50.7
HallusionBench	39.2	38.5	42.7	43.5	45.5	49.0
OCRBench	794	773	800	764	831	843
MME	1872	1813	2091	1715	1866	1850
SEEDBench	71.5	78.9	73.2	73.6	73.6	74.5
Average	60.2	62.6	63.6	62.4	64.0	64.8

Table 2: Performance comparison with state-of-the-art lightweight MLLMs on 11 common VLM benchmarks. For average score calculation, MME’s score is normalized by dividing it with 28 and OCRBench’s score is divided by 10 (same for below). s: static resolution, d: dynamic tiling w/o ISS, d-ISS: dynamic tiling w/ ISS.

4.3 Comparison of ViTs

We give the VLM performance comparison under the ablation setting (Section 4.1) in Table 3 when choosing AIMv2 [19] and SigLIP2 [74] as visual encoders, all with static input resolutions. SigLIP2 generally demonstrates a richer power of visual representation, which transfers well on multiple VLM tasks. As shown in Table 3, SigLIP2-so400m@512 achieves the state-of-the-art performance with an average score of 50.0%, a +3.10% improvement over AIMv2-H/14@448, surpassing SigLIP2-L/16@384. Notably, on OCRBench, SigLIP2-so400m@512 achieves leading performance compared with AIMv2-H/14@448 (e.g. 386 vs. 184). We also conduct ablation experiments on dynamic resolution when choosing AIMv2 and SigLIP2 as visual encoders in Table 10 of Section A.3, we find that dynamic resolution has a negative impact when using SigLIP2, which is left for future study.

Benchmark	AIMv2-H/14@448	SigLIP2-L/16@384	SigLIP2-so400m@512
visual tokens	256	144	256
MMMU _{val}	40.3	38.8	38.8 (-1.5)
MMBench ^{en}	68.2	69.0	71.7 (+3.5)
MMBench ^{cn}	66.4	67.5	68.2 (+1.8)
MMStar	43.3	41.5	43.3 (+0.0)
MathVista _{testmini}	27.9	27.8	27.9 (+0.0)
AI2D _{test}	60.0	60.1	62.3 (+2.3)
MMVet	33.8	32.4	34.4 (+0.6)
HallusionBench	34.8	38.3	39.8 (+5.0)
OCRBench	184	342	386 (+202)
MME	1505	1557	1531 (+26)
SEEDBench	69.1	69.1	70.7 (+1.6)
Average	46.9	48.6	50.0 (+3.1)

Table 3: Comparison with various vision encoders on 11 common VLM benchmarks. +/- are based on AIMv2-H/14@448.

4.4 Ablation Study of DPO

As shown in Table 4, Flash-VL-2B_s, Flash-VL-2B_d, and Flash-VL-2B_{d-ISS} all achieve superior performance compared with their pre-DPO counterparts. Notably, on OCRBench, the score rises from 696 to 764 for Flash-VL-2B_s, from 786 to 831 for Flash-VL-2B_d, and from 795 to 843 on the Flash-VL-2B_{d-ISS}. As per MMVet, the score significantly improves from 40.4 to 47.3 for Flash-VL-2B_s, from 48.1 to 52.7 for Flash-VL-2B_d, and from 45.5 to 50.7 for Flash-VL-2B_{d-ISS}. These results highlight the effectiveness of the curated DPO dataset and the training scheme in enhancing multimodal capabilities.

Benchmark	Flash-VL-2B _s	Flash-VL-2B _s -DPO	Flash-VL-2B _d	Flash-VL-2B _d -DPO	Flash-VL-2B _d -ISS	Flash-VL-2B _d -ISS-DPO
MMMU _{val}	40.8	43.6 (+2.8)	43.3	42.9 (-0.4)	40.7	42.9 (+2.2)
MMBench ^{en}	76.7	78.4 (+1.7)	76.5	78.4 (+1.9)	77.8	79.1 (+1.3)
MMBench ^{cn}	74.1	74.7 (+0.6)	74.7	74.9 (+0.2)	75.0	76.7 (+1.7)
MMStar	53.4	53.8 (+0.4)	54.3	54.4 (+0.1)	55.0	54.1 (-0.9)
MathVista _{testmini}	56.1	59.3 (+3.2)	54.7	58.1 (+3.4)	62.0	61.5 (-0.5)
AI2D _{test}	73.6	74.1 (+0.5)	74.1	74.1 (+0.0)	75.2	74.4 (-0.8)
MMVet	40.4	47.3 (+6.9)	48.1	52.7 (+4.6)	45.5	50.7 (+5.2)
HallusionBench	44.6	43.5 (-1.1)	43.4	45.5 (+2.1)	47.6	49.0 (+1.4)
OCRBench	696	764 (+68)	786	831 (+45)	795	843 (+48)
MME	1804	1715 (-89)	1910	1866 (-44)	1894	1850 (-44)
SEEDBench	73.2	73.6 (+0.4)	73.3	73.6 (+0.3)	74.4	74.5 (+0.1)
Average	60.6	62.4 (+1.8)	62.7	64.0 (+1.3)	63.7	64.8 (+1.1)

Table 4: Ablation study using DPO dataset on Flash-VL-2B_s, Flash-VL-2B_d and Flash-VL-2B_d-ISS.

4.5 Multi-stage Training

Table 5 illustrates the performance after each stage of training Flash-VL-2B with the static resolution strategy. We observe that the average scores indicate a consistent improvement in performance as the training data scales. Note that as we gradually introduce higher-quality data and more challenging questions, the overall performance can be consequently enhanced.

Benchmark	Stage 1	Stage 2	Stage 3	Stage 4	Stage 5
MMMU _{val}	38.8	41.3	42.0	40.8	43.6
MMBench ^{en}	67.4	70.2	74.4	76.7	78.4
MMBench ^{cn}	66.1	65.8	70.9	74.1	74.7
MMStar	41.9	44.6	51.5	53.4	53.8
MathVista _{testmini}	27.8	45.7	55.1	56.1	59.3
AI2D _{test}	62.2	66.9	72.9	73.6	74.1
MMVet	32.6	38.3	38.0	40.4	47.3
HallusionBench	38.4	39.7	39.6	44.6	43.5
OCRBench	365	563	685	696	764
MME	1499	1623	1778	1804	1715
SEEDBench	69.9	71.3	72.5	73.2	73.6
Average	48.6	54.4	59.0	60.6	62.4

Table 5: Data Scaling Performance of Flash-VL-2B at multiple training stages. The checkpoint at Stage 1 is fine-tuned with LLaVA-1.5-665K to have instruction following capabilities.

4.6 Comparison of Different Image Cropping Strategies

Table 6 compares the VLM performance of different image cropping methods mentioned in Figure 3 under the ablation setting (Section 4.1). All experiments adopt AIMv2 (H/14@448) as the vision encoder and Qwen-2.5-1.5B as the language model. We can find that the overlapping cropping strategy drops by 0.80% compared with the non-overlapping version. In contrast, our proposed ISS can further improve by 0.7% compared with dynamic cropping. For the full training of Flash-VL, the same strategy helps Flash-VL-2B_d-ISS to improve by 0.8% as shown in Table 2. Notably, the dynamic overlapping cropping strategy severely impaired the OCR and document understanding capabilities (383 vs. 366 on OCRBench). In contrast, ISS increases OCRBench from 383 to 427. This observation suggests that a large amount of repetitive information can degrade the performance, while ISS can mitigate the shortcomings of dynamic cropping by providing semantic consistency.

4.7 Comparison of Multimodal Reasoning Capacity

We conduct a series of comparative experiments to explore the effect of lightweight supervised fine-tuning (SFT) and reinforcement learning (RL) on enhancing the model’s reasoning capabilities

Method	Static	Dynamic Cropping	Dynamic Overlapping Cropping	Implicit Semantic Stitching
MMMU _{val}	40.3	39.6	39.0 (-0.6)	40.4 (+0.8)
MMBench ^{en}	68.2	71.8	70.1 (-0.7)	72.8 (+1.0)
MMBench ^{cn}	66.4	70.4	68.4 (-2.0)	70.2 (-0.2)
MMStar	43.3	42.2	44.9 (+2.7)	45.1 (+2.9)
MathVista _{testmini}	27.9	28.4	27.6 (-0.8)	28.5 (+0.1)
AI2D _{test}	60.0	63.2	62.1 (-1.1)	63.2 (+0.0)
MMVet	33.8	35.2	33.8 (-1.4)	33.9 (-1.3)
HallusionBench	34.8	36.3	36.7 (+0.4)	35.3 (-1.0)
OCRBench	184	383	366 (-17)	427 (+44)
MME	1505	1697	1601 (-96)	1687 (-10)
SeedBench	69.1	71.4	72.1 (+0.7)	72.5 (+1.1)
Average	46.9	50.6	49.9 (-0.7)	51.4 (+0.8)

Table 6: Comparison of various image processing methods. +/- are based on Dynamic Dropping.

without relying on a long chain of thoughts. We use the stage 4 model of Flash-VL-2B_s as the baseline and evaluate the effect of SFT, RL, and their combination on top of it. Specifically, we use LoRA [28] for SFT and GRPO [61] for RL. We evaluate the trained models on multiple mainstream mathematical and scientific reasoning benchmark datasets, with the average performance and subcategory results summarized in Table 7. More training settings are detailed in Section B.

We find that both lightweight supervised fine-tuning and reinforcement learning, when applied individually, significantly improve the model’s performance on mathematical reasoning tasks. Moreover, combining SFT and RL further enhances the model’s reasoning ability. The combination of SFT and RL lead to optimal average performance across all major mathematical reasoning benchmarks, effectively demonstrating the complementarity and synergistic benefits of these two methods.

Method	Average	DynaMath	MathVision	MathVerse	MMMU Pro	WeMath
Flash-VL-2B _s	23.80	23.19	26.72	16.84	16.24	36.03
+ SFT	26.08 (+2.28)	28.28	31.06	16.97	15.95	38.16
+ RL	27.23 (+3.43)	26.94	27.94	17.73	16.99	46.55
+ SFT + RL	29.05 (+5.25)	30.61	32.48	18.45	16.53	47.18

Table 7: Comparison of Flash-VL-2B_s and its variants on mathematical and reasoning benchmarks.

4.8 Comparison on Latency and Throughput

We compare our model with state-of-the-art models in terms of latency and throughput. We benchmark all the models on an NVIDIA L40 GPU using transformers with all samples from MMMU and the number of output tokens set to 128. The result is shown in Figure 1. Thanks to the architecture choices and image encoding strategies, Flash-VL-2B_s leads in the throughput, striking the highest tokens per second (60.73). The whole Flash-VL-2B series forms a new Pareto-front in the realm of VLM models of 2B parameters. We also give the comparison of latency distributions in A.4.

5 Conclusion

Motivated by stringent deployment requirements for VLMs, we construct a lightweight Flash-VL to strike a trade-off between latency and performance. Specifically, we exploit compact visual representation, effective token compression, and a powerful LLM component to build up our VLM. We also make use of the high-quality open-source multi-modal data collection as our training data. We adopt a multi-stage training pipeline that enhances its abilities gradually. Our competitive results attests that by adopting open-source models and datasets with latency constraints in mind, we can produce ultra-fast models with high performance. We hope our release could help advance the field of lightweight MLLMs.

References

- [1] Marah Abdin, Jyoti Aneja, Hany Awadalla, Ahmed Awadallah, Ammar Ahmad Awan, Nguyen Bach, Amit Bahree, Arash Bakhtiari, Jianmin Bao, Harkirat Behl, et al. Phi-3 technical report: A highly capable language model locally on your phone. *arXiv preprint arXiv:2404.14219*, 2024.
- [2] Abdelrahman Abouelenin, Atabak Ashfaq, Adam Atkinson, Hany Awadalla, Nguyen Bach, Jianmin Bao, Alon Benhaim, Martin Cai, Vishrav Chaudhary, Congcong Chen, et al. Phi-4-mini technical report: Compact yet powerful multimodal language models via mixture-of-loras. *arXiv preprint arXiv:2503.01743*, 2025.
- [3] Jinze Bai, Shuai Bai, Yunfei Chu, Zeyu Cui, Kai Dang, Xiaodong Deng, Yang Fan, Wenbin Ge, Yu Han, Fei Huang, et al. Qwen technical report. *arXiv preprint arXiv:2309.16609*, 2023.
- [4] Jinze Bai, Shuai Bai, Shusheng Yang, Shijie Wang, Sinan Tan, Peng Wang, Junyang Lin, Chang Zhou, and Jingren Zhou. Qwen-vl: A versatile vision-language model for understanding, localization, text reading, and beyond. *arXiv preprint arXiv:2308.12966*, 2023.
- [5] Guiming Hardy Chen, Shunian Chen, Ruifei Zhang, Junying Chen, Xiangbo Wu, Zhiyi Zhang, Zhihong Chen, Jianquan Li, Xiang Wan, and Benyou Wang. Allava: Harnessing gpt4v-synthesized data for a lite vision-language model, 2024.
- [6] Lin Chen, Jinsong Li, Xiaoyi Dong, Pan Zhang, Conghui He, Jiaqi Wang, Feng Zhao, and Dahua Lin. Sharegpt4v: Improving large multi-modal models with better captions. In *European Conference on Computer Vision*, pages 370–387. Springer, 2024.
- [7] Lin Chen, Jinsong Li, Xiaoyi Dong, Pan Zhang, Yuhang Zang, Zehui Chen, Haodong Duan, Jiaqi Wang, Yu Qiao, Dahua Lin, et al. Are we on the right way for evaluating large vision-language models? *arXiv preprint arXiv:2403.20330*, 2024.
- [8] Wenhui Chen, Hongmin Wang, Jianshu Chen, Yunkai Zhang, Hong Wang, Shiyang Li, Xiyu Zhou, and William Yang Wang. Tabfact: A large-scale dataset for table-based fact verification. *arXiv preprint arXiv:1909.02164*, 2019.
- [9] Zhe Chen, Weiyun Wang, Hao Tian, Shenglong Ye, Zhangwei Gao, Erfei Cui, Wenwen Tong, Kongzhi Hu, Jiapeng Luo, Zheng Ma, et al. How far are we to gpt-4v? closing the gap to commercial multimodal models with open-source suites. *arXiv preprint arXiv:2404.16821*, 2024.
- [10] Zhe Chen, Jiannan Wu, Wenhui Wang, Weijie Su, Guo Chen, Sen Xing, Muyan Zhong, Qinglong Zhang, Xizhou Zhu, Lewei Lu, et al. Internvl: Scaling up vision foundation models and aligning for generic visual-linguistic tasks. In *Proceedings of the IEEE/CVF Conference on Computer Vision and Pattern Recognition*, pages 24185–24198, 2024.
- [11] Xiangxiang Chu, Limeng Qiao, Xinyang Lin, Shuang Xu, Yang Yang, Yiming Hu, Fei Wei, Xinyu Zhang, Bo Zhang, Xiaolin Wei, et al. Mobilevlm: A fast, strong and open vision language assistant for mobile devices. *arXiv preprint arXiv:2312.16886*, 2023.
- [12] Xiangxiang Chu, Limeng Qiao, Xinyu Zhang, Shuang Xu, Fei Wei, Yang Yang, Xiaofei Sun, Yiming Hu, Xinyang Lin, Bo Zhang, et al. Mobilevlm v2: Faster and stronger baseline for vision language model. *arXiv preprint arXiv:2402.03766*, 2024.
- [13] ShengYu Shen Jialiang Peng Xiaoli Zhang ZhenDong Du YaFang Wang Cong Liu, Zhong Wang. The chinese dataset distilled from deepseek-r1-671b. <https://huggingface.co/datasets/Congliu/Chinese-DeepSeek-R1-Distill-data-110k>, 2025.
- [14] Hongyuan Dong, Zijian Kang, Weijie Yin, Xiao Liang, Chao Feng, and Jiao Ran. Scalable vision language model training via high quality data curation. *arXiv preprint arXiv:2501.05952*, 2025.
- [15] Alexey Dosovitskiy, Lucas Beyer, Alexander Kolesnikov, Dirk Weissenborn, Xiaohua Zhai, Thomas Unterthiner, Mostafa Dehghani, Matthias Minderer, Georg Heigold, Sylvain Gelly, et al. An image is worth 16x16 words: Transformers for image recognition at scale. *arXiv preprint arXiv:2010.11929*, 2020.
- [16] Haodong Duan, Junming Yang, Yuxuan Qiao, Xinyu Fang, Lin Chen, Yuan Liu, Xiaoyi Dong, Yuhang Zang, Pan Zhang, Jiaqi Wang, et al. Vlmevalkit: An open-source toolkit for evaluating large multi-modality models. In *Proceedings of the 32nd ACM International Conference on Multimedia*, pages 11198–11201, 2024.
- [17] Alaaeldin El-Nouby, Michal Klein, Shuangfei Zhai, Miguel Angel Bautista, Alexander Toshev, Vaishal Shankar, Joshua M Susskind, and Armand Joulin. Scalable pre-training of large autoregressive image models. *arXiv preprint arXiv:2401.08541*, 2024.
- [18] Alex Fang, Albin Madappally Jose, Amit Jain, Ludwig Schmidt, Alexander Toshev, and Vaishal Shankar. Data filtering networks. *arXiv preprint arXiv:2309.17425*, 2023.
- [19] Enrico Fini, Mustafa Shukor, Xiujun Li, Philipp Dufter, Michal Klein, David Haldimann, Sai Aitharaju, Victor Guilherme Turrissi da Costa, Louis Béthune, Zhe Gan, et al. Multimodal autoregressive pre-training of large vision encoders. *arXiv preprint arXiv:2411.14402*, 2024.

- [20] Chaoyou Fu, Peixian Chen, Yunhang Shen, Yulei Qin, Mengdan Zhang, Xu Lin, Jinrui Yang, Xiawu Zheng, Ke Li, Xing Sun, et al. Mme: A comprehensive evaluation benchmark for multimodal large language models. *arXiv preprint arXiv:2306.13394*, 2023.
- [21] Samir Yitzhak Gadre, Gabriel Ilharco, Alex Fang, Jonathan Hayase, Georgios Smyrnis, Thao Nguyen, Ryan Marten, Mitchell Wortsman, Dhruva Ghosh, Jieyu Zhang, et al. Datacomp: In search of the next generation of multimodal datasets. *Advances in Neural Information Processing Systems*, 36:27092–27112, 2023.
- [22] Aaron Grattafiori, Abhimanyu Dubey, Abhinav Jauhri, Abhinav Pandey, Abhishek Kadian, Ahmad Al-Dahle, Aiesha Letman, Akhil Mathur, Alan Schelten, Alex Vaughan, et al. The llama 3 herd of models. *arXiv preprint arXiv:2407.21783*, 2024.
- [23] Shuhao Gu, Jialing Zhang, Siyuan Zhou, Kevin Yu, Zhaohu Xing, Liangdong Wang, Zhou Cao, Jintao Jia, Zhuoyi Zhang, Yixuan Wang, Zhenchong Hu, Bo-Wen Zhang, Jijie Li, Dong Liang, Yingli Zhao, Yulong Ao, Yaoqi Liu, Fangxiang Feng, and Guang Liu. Infinity-mm: Scaling multimodal performance with large-scale and high-quality instruction data, 2024.
- [24] Tianrui Guan, Fuxiao Liu, Xiyang Wu, Ruiqi Xian, Zongxia Li, Xiaoyu Liu, Xijun Wang, Lichang Chen, Furong Huang, Yaser Yacoob, et al. Hallusionbench: an advanced diagnostic suite for entangled language hallucination and visual illusion in large vision-language models. In *Proceedings of the IEEE/CVF Conference on Computer Vision and Pattern Recognition*, pages 14375–14385, 2024.
- [25] Suriya Gunasekar, Yi Zhang, Jyoti Aneja, Caio César Teodoro Mendes, Allie Del Giorno, Sivakanth Gopi, Mojan Javaheripi, Piero Kauffmann, Gustavo de Rosa, Olli Saarikivi, et al. Textbooks are all you need. *arXiv preprint arXiv:2306.11644*, 2023.
- [26] Guiming Hardy Chen, Shunian Chen, Ruifei Zhang, Junying Chen, Xiangbo Wu, Zhiyi Zhang, Zhihong Chen, Jianquan Li, Xiang Wan, and Benyou Wang. Allava: Harnessing gpt4v-synthesized data for a lite vision-language model. *arXiv e-prints*, pages arXiv–2402, 2024.
- [27] Anwen Hu, Haiyang Xu, Jiabo Ye, Ming Yan, Liang Zhang, Bo Zhang, Chen Li, Ji Zhang, Qin Jin, Fei Huang, et al. mplug-docowl 1.5: Unified structure learning for ocr-free document understanding. *arXiv preprint arXiv:2403.12895*, 2024.
- [28] Edward J Hu, Yelong Shen, Phillip Wallis, Zeyuan Allen-Zhu, Yuanzhi Li, Shean Wang, Lu Wang, Weizhu Chen, et al. Lora: Low-rank adaptation of large language models. *ICLR*, 1(2):3, 2022.
- [29] Shengding Hu, Yuge Tu, Xu Han, Chaoqun He, Ganqu Cui, Xiang Long, Zhi Zheng, Yewei Fang, Yuxiang Huang, Weilin Zhao, et al. Minicpm: Unveiling the potential of small language models with scalable training strategies. *arXiv preprint arXiv:2404.06395*, 2024.
- [30] Aniruddha Kembhavi, Mike Salvato, Eric Kolve, Minjoon Seo, Hannaneh Hajishirzi, and Ali Farhadi. A diagram is worth a dozen images. In *Computer Vision—ECCV 2016: 14th European Conference, Amsterdam, The Netherlands, October 11–14, 2016, Proceedings, Part IV 14*, pages 235–251. Springer, 2016.
- [31] Woosuk Kwon, Zhuohan Li, Siyuan Zhuang, Ying Sheng, Lianmin Zheng, Cody Hao Yu, Joseph E. Gonzalez, Hao Zhang, and Ion Stoica. Efficient memory management for large language model serving with pagedattention. In *Proceedings of the ACM SIGOPS 29th Symposium on Operating Systems Principles*, 2023.
- [32] Hugo Laurençon, Léo Tronchon, and Victor Sanh. Unlocking the conversion of web screenshots into html code with the websight dataset. *arXiv preprint arXiv:2403.09029*, 2024.
- [33] Bo Li, Yuanhan Zhang, Dong Guo, Renrui Zhang, Feng Li, Hao Zhang, Kaichen Zhang, Peiyuan Zhang, Yanwei Li, Ziwei Liu, et al. Llava-onevision: Easy visual task transfer. *arXiv preprint arXiv:2408.03326*, 2024.
- [34] Bohao Li, Rui Wang, Guangzhi Wang, Yuying Ge, Yixiao Ge, and Ying Shan. Seed-bench: Benchmarking multimodal llms with generative comprehension. *arXiv preprint arXiv:2307.16125*, 2023.
- [35] Feng Li, Renrui Zhang, Hao Zhang, Yuanhan Zhang, Bo Li, Wei Li, Zejun Ma, and Chunyuan Li. Llava-next-interleave: Tackling multi-image, video, and 3d in large multimodal models. *arXiv preprint arXiv:2407.07895*, 2024.
- [36] Lei Li, Zhihui Xie, Mukai Li, Shunian Chen, Peiyi Wang, Liang Chen, Yazheng Yang, Benyou Wang, Lingpeng Kong, and Qi Liu. Vfeedback: A large-scale ai feedback dataset for large vision-language models alignment. *arXiv preprint arXiv:2410.09421*, 2024.
- [37] Lei Li, Yuwei Yin, Shicheng Li, Liang Chen, Peiyi Wang, Shuhuai Ren, Mukai Li, Yazheng Yang, Jingjing Xu, Xu Sun, et al. M3 it: A large-scale dataset towards multi-modal multilingual instruction tuning. *arXiv preprint arXiv:2306.04387*, 2023.
- [38] Shengzhi Li and Nima Tajbakhsh. Scigraphqa: A large-scale synthetic multi-turn question-answering dataset for scientific graphs. *arXiv preprint arXiv:2308.03349*, 2023.

- [39] Yuanzhi Li, Sébastien Bubeck, Ronen Eldan, Allie Del Giorno, Suriya Gunasekar, and Yin Tat Lee. Textbooks are all you need ii: phi-1.5 technical report. *arXiv preprint arXiv:2309.05463*, 2023.
- [40] Haotian Liu, Chunyuan Li, Yuheng Li, and Yong Jae Lee. Improved baselines with visual instruction tuning, 2023.
- [41] Haotian Liu, Chunyuan Li, Qingyang Wu, and Yong Jae Lee. Visual instruction tuning, 2023.
- [42] Yuliang Liu, Zhang Li, Mingxin Huang, Biao Yang, Wenwen Yu, Chunyuan Li, Xu-Cheng Yin, Cheng-Lin Liu, Lianwen Jin, and Xiang Bai. Ocrbench: on the hidden mystery of ocr in large multimodal models. *Science China Information Sciences*, 67(12):220102, 2024.
- [43] Zhijian Liu, Ligeng Zhu, Baifeng Shi, Zhuoyang Zhang, Yuming Lou, Shang Yang, Haocheng Xi, Shiyi Cao, Yuxian Gu, Dacheng Li, et al. Nvila: Efficient frontier visual language models. *arXiv preprint arXiv:2412.04468*, 2024.
- [44] Ziyu Liu, Tao Chu, Yuhang Zang, Xilin Wei, Xiaoyi Dong, Pan Zhang, Zijian Liang, Yuanjun Xiong, Yu Qiao, Dahua Lin, et al. Mmdu: A multi-turn multi-image dialog understanding benchmark and instruction-tuning dataset for lvlms. *arXiv preprint arXiv:2406.11833*, 2024.
- [45] LMMs-Lab. multimodal-open-r1-8k-verified. <https://huggingface.co/datasets/lmms-lab/multimodal-open-r1-8k-verified>, 2024.
- [46] Pan Lu, Hritik Bansal, Tony Xia, Jiacheng Liu, Chunyuan Li, Hannaneh Hajishirzi, Hao Cheng, Kai-Wei Chang, Michel Galley, and Jianfeng Gao. Mathvista: Evaluating mathematical reasoning of foundation models in visual contexts. *arXiv preprint arXiv:2310.02255*, 2023.
- [47] Xinyin Ma, Gongfan Fang, and Xinchao Wang. Llm-pruner: On the structural pruning of large language models. In *Advances in Neural Information Processing Systems*, 2023.
- [48] Ahmed Masry, Do Xuan Long, Jia Qing Tan, Shafiq Joty, and Enamul Hoque. Chartqa: A benchmark for question answering about charts with visual and logical reasoning. *arXiv preprint arXiv:2203.10244*, 2022.
- [49] Minesh Mathew, Viraj Bagal, Rubèn Tito, Dimosthenis Karatzas, Ernest Valveny, and CV Jawahar. Infographicvqa. In *Proceedings of the IEEE/CVF Winter Conference on Applications of Computer Vision*, pages 1697–1706, 2022.
- [50] Minesh Mathew, Dimosthenis Karatzas, and CV Jawahar. Docvqa: A dataset for vqa on document images. In *Proceedings of the IEEE/CVF winter conference on applications of computer vision*, pages 2200–2209, 2021.
- [51] Saurav Muralidharan, Sharath Turuvekere Sreenivas, Raviraj Joshi, Marcin Chochowski, Mostofa Patwary, Mohammad Shoeybi, Bryan Catanzaro, Jan Kautz, and Pavlo Molchanov. Compact language models via pruning and knowledge distillation. *Advances in Neural Information Processing Systems*, 37:41076–41102, 2024.
- [52] Maxime Oquab, Timothée Darcet, Théo Moutakanni, Huy Vo, Marc Szafranec, Vasil Khalidov, Pierre Fernandez, Daniel Haziza, Francisco Massa, Alaaeldin El-Nouby, et al. Dinov2: Learning robust visual features without supervision. *arXiv preprint arXiv:2304.07193*, 2023.
- [53] Panupong Pasupat and Percy Liang. Compositional semantic parsing on semi-structured tables. *arXiv preprint arXiv:1508.00305*, 2015.
- [54] Shuai Peng, Di Fu, Liangcai Gao, Xiuqin Zhong, Hongguang Fu, and Zhi Tang. Multimath: Bridging visual and mathematical reasoning for large language models. *arXiv preprint arXiv:2409.00147*, 2024.
- [55] Ofir Press and Lior Wolf. Using the output embedding to improve language models. *arXiv preprint arXiv:1608.05859*, 2016.
- [56] Runqi Qiao, Qiuna Tan, Guanting Dong, Minhui Wu, Chong Sun, Xiaoshuai Song, Zhuoma GongQue, Shanglin Lei, Zhe Wei, Miaoxuan Zhang, Runfeng Qiao, Yifan Zhang, Xiao Zong, Yida Xu, Muxi Diao, Zhimin Bao, Chen Li, and Honggang Zhang. We-math: Does your large multimodal model achieve human-like mathematical reasoning?, 2024.
- [57] Alec Radford, Jong Wook Kim, Chris Hallacy, Aditya Ramesh, Gabriel Goh, Sandhini Agarwal, Girish Sastry, Amanda Askell, Pamela Mishkin, Jack Clark, et al. Learning transferable visual models from natural language supervision. In *International conference on machine learning*, pages 8748–8763. PmlR, 2021.
- [58] Rafael Rafailov, Archit Sharma, Eric Mitchell, Christopher D Manning, Stefano Ermon, and Chelsea Finn. Direct preference optimization: Your language model is secretly a reward model. *Advances in Neural Information Processing Systems*, 36:53728–53741, 2023.
- [59] S. A. Laboratory. ShareGPT-4o. <https://sharegpt4o.github.io/>, 2024.
- [60] sgl project. Sglang: A fast serving framework for large language models and vision language models. <https://github.com/sgl-project/sglang>, 2024. Accessed: 2025-05-14.

- [61] Zhihong Shao, Peiyi Wang, Qihao Zhu, Runxin Xu, Junxiao Song, Xiao Bi, Haowei Zhang, Mingchuan Zhang, YK Li, Y Wu, et al. Deepseekmath: Pushing the limits of mathematical reasoning in open language models. *arXiv preprint arXiv:2402.03300*, 2024.
- [62] Noam Shazeer. Glu variants improve transformer. *arXiv preprint arXiv:2002.05202*, 2020.
- [63] Oleksii Sidorov, Ronghang Hu, Marcus Rohrbach, and Amanpreet Singh. Textcaps: a dataset for image captioning with reading comprehension. In *Computer Vision—ECCV 2020: 16th European Conference, Glasgow, UK, August 23–28, 2020, Proceedings, Part II 16*, pages 742–758. Springer, 2020.
- [64] Amanpreet Singh, Vivek Natarajan, Meet Shah, Yu Jiang, Xinlei Chen, Dhruv Batra, Devi Parikh, and Marcus Rohrbach. Towards vqa models that can read. In *Proceedings of the IEEE/CVF conference on computer vision and pattern recognition*, pages 8317–8326, 2019.
- [65] Tomasz Stanisławek, Filip Graliński, Anna Wróblewska, Dawid Lipiński, Agnieszka Kaliska, Paulina Rosalska, Bartosz Topolski, and Przemysław Biecek. Kleister: key information extraction datasets involving long documents with complex layouts. In *International Conference on Document Analysis and Recognition*, pages 564–579. Springer, 2021.
- [66] Jianlin Su, Murtadha Ahmed, Yu Lu, Shengfeng Pan, Wen Bo, and Yunfeng Liu. Roformer: Enhanced transformer with rotary position embedding. *Neurocomputing*, 568:127063, 2024.
- [67] Quan Sun, Yuxin Fang, Ledell Wu, Xinlong Wang, and Yue Cao. Eva-clip: Improved training techniques for clip at scale. *arXiv preprint arXiv:2303.15389*, 2023.
- [68] S. Svetlichnaya. Deepform: Understand structured documents at scale. https://wandb.ai/stacey/deepform_v1/reports/DeepForm-Understand-Structured-Documents-at-Scale--VmlldzoyODQ3Njg, 2020.
- [69] Ryota Tanaka, Kyosuke Nishida, and Sen Yoshida. Visualmrc: Machine reading comprehension on document images. In *Proceedings of the AAAI Conference on Artificial Intelligence*, volume 35, pages 13878–13888, 2021.
- [70] Gemma Team, Aishwarya Kamath, Johan Ferret, Shreya Pathak, Nino Vieillard, Ramona Merhej, Sarah Perrin, Tatiana Matejovicova, Alexandre Ramé, Morgane Rivière, et al. Gemma 3 technical report. *arXiv preprint arXiv:2503.19786*, 2025.
- [71] Gemma Team, Morgane Riviere, Shreya Pathak, Pier Giuseppe Sessa, Cassidy Hardin, Surya Bhupatiraju, Léonard Hussenot, Thomas Mesnard, Bobak Shahriari, Alexandre Ramé, et al. Gemma 2: Improving open language models at a practical size. *arXiv preprint arXiv:2408.00118*, 2024.
- [72] Hugo Touvron, Thibaut Lavril, Gautier Izacard, Xavier Martinet, Marie-Anne Lachaux, Timothée Lacroix, Baptiste Rozière, Naman Goyal, Eric Hambro, Faisal Azhar, et al. Llama: Open and efficient foundation language models. *arXiv preprint arXiv:2302.13971*, 2023.
- [73] Hugo Touvron, Louis Martin, Kevin Stone, Peter Albert, Amjad Almahairi, Yasmine Babaei, Nikolay Bashlykov, Soumya Batra, Prajjwal Bhargava, Shruti Bhosale, et al. Llama 2: Open foundation and fine-tuned chat models. *arXiv preprint arXiv:2307.09288*, 2023.
- [74] Michael Tschannen, Alexey Gritsenko, Xiao Wang, Muhammad Ferjad Naeem, Ibrahim Alabdulmohsin, Nikhil Parthasarathy, Talfan Evans, Lucas Beyer, Ye Xia, Basil Mustafa, et al. Siglip 2: Multilingual vision-language encoders with improved semantic understanding, localization, and dense features. *arXiv preprint arXiv:2502.14786*, 2025.
- [75] Pavan Kumar Anasosalu Vasu, Fartash Faghri, Chun-Liang Li, Cem Koc, Nate True, Albert Antony, Gokul Santhanam, James Gabriel, Peter Grasch, Oncel Tuzel, et al. Fastvlm: Efficient vision encoding for vision language models. *arXiv preprint arXiv:2412.13303*, 2024.
- [76] Bo Wan, Michael Tschannen, Yongqin Xian, Filip Pavetic, Ibrahim M Alabdulmohsin, Xiao Wang, André Susano Pinto, Andreas Steiner, Lucas Beyer, and Xiaohua Zhai. Locca: Visual pretraining with location-aware captioners. *Advances in Neural Information Processing Systems*, 37:116355–116387, 2024.
- [77] Ke Wang, Junting Pan, Weikang Shi, Zimu Lu, Houxing Ren, Aojun Zhou, Mingjie Zhan, and Hongsheng Li. Measuring multimodal mathematical reasoning with math-vision dataset. In *The Thirty-eight Conference on Neural Information Processing Systems Datasets and Benchmarks Track*, 2024.
- [78] Peng Wang, Shuai Bai, Sinan Tan, Shijie Wang, Zhihao Fan, Jinze Bai, Keqin Chen, Xuejing Liu, Jialin Wang, Wenbin Ge, Yang Fan, Kai Dang, Mengfei Du, Xuancheng Ren, Rui Men, Dayiheng Liu, Chang Zhou, Jingren Zhou, and Junyang Lin. Qwen2-vl: Enhancing vision-language model’s perception of the world at any resolution. *arXiv preprint arXiv:2409.12191*, 2024.
- [79] Zhiyu Wu, Xiaokang Chen, Zizheng Pan, Xingchao Liu, Wen Liu, Damai Dai, Huazuo Gao, Yiyang Ma, Chengyue Wu, Bingxuan Wang, Zhenda Xie, Yu Wu, Kai Hu, Jiawei Wang, Yaofeng Sun, Yukun Li, Yishi Piao, Kang Guan, Aixin Liu, Xin Xie, Yuxiang You, Kai Dong, Xingkai Yu, Haowei Zhang, Liang Zhao, Yisong Wang, and Chong Ruan. Deepseek-vl2: Mixture-of-experts vision-language models for advanced multimodal understanding, 2024.

- [80] An Yang, Baosong Yang, Beichen Zhang, Binyuan Hui, Bo Zheng, Bowen Yu, Chengyuan Li, Dayiheng Liu, Fei Huang, Haoran Wei, et al. Qwen2. 5 technical report. *arXiv preprint arXiv:2412.15115*, 2024.
- [81] An Yang, Baosong Yang, Beichen Zhang, Binyuan Hui, Bo Zheng, Bowen Yu, Chengyuan Li, Dayiheng Liu, Fei Huang, Haoran Wei, Huan Lin, Jian Yang, Jianhong Tu, Jianwei Zhang, Jianxin Yang, Jiayi Yang, Jingren Zhou, Junyang Lin, Kai Dang, Keming Lu, Keqin Bao, Kexin Yang, Le Yu, Mei Li, Mingfeng Xue, Pei Zhang, Qin Zhu, Rui Men, Runji Lin, Tianhao Li, Tingyu Xia, Xingzhang Ren, Xuancheng Ren, Yang Fan, Yang Su, Yichang Zhang, Yu Wan, Yuqiong Liu, Zeyu Cui, Zhenru Zhang, and Zihan Qiu. Qwen2.5 technical report. *arXiv preprint arXiv:2412.15115*, 2024.
- [82] Weihao Yu, Zhengyuan Yang, Linjie Li, Jianfeng Wang, Kevin Lin, Zicheng Liu, Xinchao Wang, and Lijuan Wang. Mm-vet: Evaluating large multimodal models for integrated capabilities. *arXiv preprint arXiv:2308.02490*, 2023.
- [83] Yuanhan Zhang Bo Li Songyang Zhang Wangbo Zhao Yike Yuan Jiaqi Wang Conghui He Ziwei Liu Kai Chen Dahua Lin Yuan Liu, Haodong Duan. Mmbench: Is your multi-modal model an all-around player? *arXiv:2307.06281*, 2023.
- [84] Xiang Yue, Yuansheng Ni, Kai Zhang, Tianyu Zheng, Ruoqi Liu, Ge Zhang, Samuel Stevens, Dongfu Jiang, Weiming Ren, Yuxuan Sun, et al. Mmmu: A massive multi-discipline multimodal understanding and reasoning benchmark for expert agi. In *Proceedings of the IEEE/CVF Conference on Computer Vision and Pattern Recognition*, pages 9556–9567, 2024.
- [85] Xiang Yue, Tianyu Zheng, Yuansheng Ni, Yubo Wang, Kai Zhang, Shengbang Tong, Yuxuan Sun, Botao Yu, Ge Zhang, Ruoqi Liu, Dongfu Jiang, Weiming Ren, Cong Wei, Ruibin Yuan, Renliang Sun, Ming Yin, Boyuan Zheng, Zhenzhu Yang, Yibo Liu, Wenhao Huang, Huan Sun, Yu Su, and Wenhui Chen. MMMU-Pro: A More Robust Multi-discipline Multimodal Understanding Benchmark. *arXiv preprint arXiv:2409.02813*, 2024.
- [86] Xiaohua Zhai, Basil Mustafa, Alexander Kolesnikov, and Lucas Beyer. Sigmoid loss for language image pre-training. In *Proceedings of the IEEE/CVF international conference on computer vision*, pages 11975–11986, 2023.
- [87] Biao Zhang and Rico Sennrich. Root mean square layer normalization. *Advances in Neural Information Processing Systems*, 32, 2019.
- [88] Renrui Zhang, Dongzhi Jiang, Yichi Zhang, Haokun Lin, Ziyu Guo, Pengshuo Qiu, Aojun Zhou, Pan Lu, Kai-Wei Chang, Jianfeng Gao, and Hongsheng Li. Mathverse: Does your multi-modal llm truly see the diagrams in visual math problems? *arXiv preprint arXiv:2403.14624*, 2024.
- [89] Renrui Zhang, Xinyu Wei, Dongzhi Jiang, Yichi Zhang, Ziyu Guo, Chengzhuo Tong, Jiaming Liu, Aojun Zhou, Bin Wei, Shanghang Zhang, et al. Mavis: Mathematical visual instruction tuning. *arXiv e-prints*, pages arXiv–2407, 2024.
- [90] Chengke Zou, Xingang Guo, Rui Yang, Junyu Zhang, Bin Hu, and Huan Zhang. Dynamath: A dynamic visual benchmark for evaluating mathematical reasoning robustness of vision language models, 2024.

A Additional Experiments and Ablations

A.1 Comparison of Adapters

Current VLMs simply utilize two MLPs (i.e. linear layer) for the adapter. We compare our proposed adapter with this simplistic design, shown in Table 8. Both adapters use pixel shuffling to compress visual tokens first. The same in-house ViT-Huge and Qwen-2-1.5B are used for ViT and LLM, respectively.

Benchmark	$2 \times$ Linear	Proposed Adapter
MMMU _{val}	36.7	38.3
MMBench ^{en}	56.5	61.5
MMBench ^{cn}	55.2	57.3
MMStar	33.6	35.7
MathVista _{testmini}	27.8	24.0
AI2D _{test}	55.2	54.6
MMVet	17.6	23.9
HallusionBench	27.6	33.7
OCRBench	54	168
MME	1436	1569
SEEDBench	55.1	62.6
Average	39.4	40.8

Table 8: VLM performance comparison of two adapter designs.

A.2 Comparison of LLMs

With an in-house contrastively-trained ViT-Huge as the same vision encoder, we evaluate the performance of various LLMs, namely LLaMA-3.2-1B (1.23B parameters), Qwen-2-1.5B and Qwen-2.5-1.5B, under the same framework and the ablation data setting. Among three candidate lightweight LLMs, Qwen-2.5-1.5B demonstrates superiority by a clear margin, shown in Table 9. Hence for the rest of experiments throughout the paper, we adopt Qwen-2.5-1.5B as the default LLM component.

Benchmark	LLaMA-3.2-1B	Qwen-2-1.5B	Qwen-2.5-1.5B
MMMU _{val}	30.3	34.8	38.3
MMBench ^{en}	41.4	62.3	61.5
MMBench ^{cn}	42.4	56.7	57.3
MMStar	28.5	35.0	35.7
MathVista _{testmini}	23.5	15.9	24.0
AI2D _{test}	54.0	52.3	54.6
MMVet	20.1	18.2	23.9
HallusionBench	29.1	28.4	33.7
OCRBench	193	195	168
MME	1324	1477	1569
SEEDBench	46.9	62.1	62.6
Average	33.2	38.3	40.8

Table 9: VLM performance comparison under various lightweight LLM choices.

A.3 Ablation of Dynamic Resolution Setting on AIMv2 and SigLIP2

Dynamic resolution, as a commonly used technique, can consistently improve model performance. We conducted ablation experiments on this technique when choosing AIMv2 and SigLIP2 as visual encoders, as shown in Table 10. Surprisingly, we discover that the dynamic setting hurts the performance on SigLIP2 while the AIMv2’s version gets substantially enhanced. We leave it here as an open discussion why feeding more visual tokens is not more effective for SigLIP2.

Benchmark	AIMv2 H/14@448	+ Dynamic Resolution	SigLIP2 so400m@512	+ Dynamic Resolution
Max Image Split	-1	4	-1	4
MMMU _{val}	40.3	39.6	38.8	39.1
MMBench ^{en}	68.2	71.8	71.7	70.5
MMBench ^{cn}	66.4	70.4	68.2	68.4
MMStar	43.3	42.2	43.3	41.8
MathVista _{testmini}	27.9	28.4	27.9	27.1
AI2D _{test}	60.0	63.2	62.3	61.0
MMVet	33.8	35.2	34.4	32.3
HallusionBench	34.8	36.3	39.8	35.4
OCRBench	184	383	386	367
MME	1505	1697	1531	1662
SEEDBench	69.1	71.4	70.7	70.8
Average	46.9	50.7	50.0	49.3

Table 10: Abatement of dynamic resolution with various vision encoders on 11 common VLM benchmarks.

A.4 Comparison of TTFT/TPOT on MMMU

Apart from benchmarking the throughputs in Figure 1, we also profile the time-to-first-token (TTFT) and the time-per-output-token (TPOT) of the state-of-the-art 2B VLM models on MMMU [84] with the official evaluation prompts in Figure 7. The number of output tokens is all set to 128. The former metric describes the prefilling latency, while the latter is about self-decoding speed. Our models exhibit the best TPOT on average. Although QwenVL-2-2B’s image processing strategy benefits a competitive TTFT (0.14s), its wider range of embedding tokens contributes to a longer decoding time, effectively slowing down the overall throughput (39.07 tokens/s) as shown in Figure 1. Thanks to our token mechanisms and the choice of a compact vision encoder, our Flash-VL-2B_s, Flash-VL-2B_d, and Flash-VL-2B_{d_{ISS}} enjoy the overall best average latencies (0.04, 0.13, 0.18 seconds on TTFT and approximately 0.015 seconds for all models on TPOT) and throughputs (60.73, 51.53, 48.66 tokens/s) out of all state-of-the-art models.

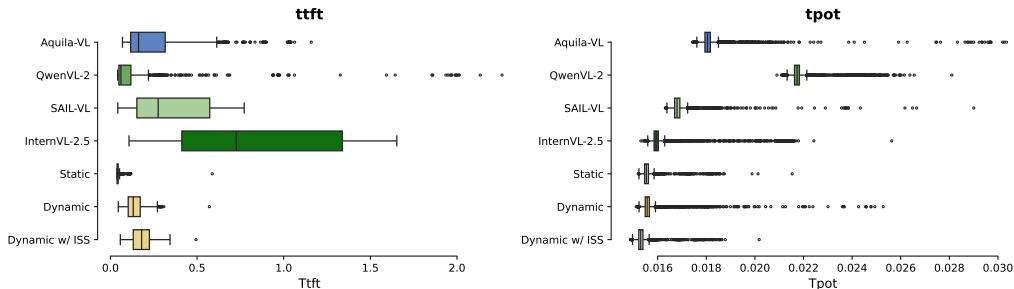


Figure 7: **Left:** Distribution of TTFT on MMMU. **Right:** Distribution of TPOT on MMMU.

B Experimental Setup for Reasoning Capacity Comparison

Here we detail the datasets and training strategies in Section 4.7.

For the SFT phase, we use the open-source distilled dataset Chinese-DeepSeek-R1-Distill-data-110k [13]. This dataset primarily targets domains such as logical and mathematical reasoning, while also encompassing a proportion of general-purpose corpora. During training, only the content field was considered as the training label, while the reasoning_content field was not utilized. We conducted SFT with the Low-Rank Adaptation (LoRA) [28] for efficient fine-tuning. The learning rate was set to 1×10^{-5} , coupled with a cosine annealing learning rate scheduler.

For the RL phase, we employ the open-source multimodal-open-r1-8k-verified [45] dataset. This is a visual multimodal dataset oriented towards geometric reasoning. The RL phase adopted GRPO [61].

Each group consists of 24 samples. The regularization coefficient β for KL divergence is set to 0.001, and the learning rate is 5×10^{-7} with a cosine annealing scheduler.

Both phases were trained for a single epoch each. The last checkpoint from the complete training was selected for final testing.

C Limitations

Although our models achieve state-of-the-art performance, which well balances the performance and speed, our overall performance might be limited by not exploiting a much larger set of in-house datasets as many closed-sourced VLMs do. Besides, the choice of standard benchmarks may not be comprehensive enough to reflect the full spectrum of VLM’s capacity. In the meantime, we leave multi-image, video processing capabilities for the next generation and don’t compare such scenarios. We also didn’t target specific hardware devices, which may still introduce difficulties when it comes to real applications. Further, industry-level inference frameworks like vLLM [31] or SGLang [60] could also be exploited to enhance the inference speed.